Northern Arizona University

2022 Collegiate Wind Competition

Turbine Team

Technical Design Report

For the United States Department of Energy

4/24/2022

Prepared by,

Owen Murphy	Mikela Petersen	Lucas Johnson	Graham Burnside	Dario DeDonato	Ben Coulter
ME Team Lead	Blades	Pitching	Foundation	Tower & Yaw	Brakes
jom28@nau.edu	mmp378@nau.edu	lbj38@nau.edu	gfb32@nau.edu	dgd53@nau.edu	bsc226@nau.edu

Samantha Nearing	Chase Hughes	Andrew Harper	Tyler Schwartz	Maxwell Fawcett
EE Team Lead	Diversion Load	DC/DC Converter	PCB Design	Arduino Control
sdn63@iris.nau.edu	cmh789@nau.edu	andrew.harper@nau.edu	tms579@nau.edu	mbf95@nau.edu

WindJa Energy Club at NAU

1 Contents

2 Executive Summary

Northern Arizona University's WindJax team designed, analyzed, and tested a micro-wind turbine and foundation system for the 2022 Collegiate Wind Competition. This report discusses the design choices that the team made, what analysis methods were used to estimate turbine performance, and the testing procedures used to validate the design.

The turbine design consists of a three bladed horizontal axis wind turbine with composite blades, an active pitching system, and a disk brake. The airfoil selected was the GOE79, and the blades were manufactured by vacuum bagging a flax seed based composite structure called BComp around 3D printed cores.

Figure 1: Wind Turbine Full CAD Model Isometric

The variable pitch design was initially based on last year's swash plate system. However, the team made multiple design changes in order to improve performance and reliability. These changes included a hub diameter reduction, swash plate size reduction, switching from a PLA bearing to stainless steel, and directly mounting a linear actuator in place of last year's rack and pinion system.

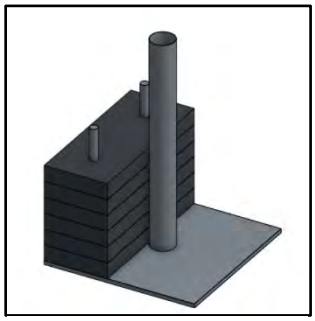

Figure 2: Foundation CAD Model

Due to the introduction of the foundation design requirements for this year's competition, the team prioritized early design prototypes and testing for this system. Additionally, significant efforts were put towards streamlining the turbine and tower to reduce drag forces. After thorough testing, the team settled on a gravity based, directional foundation design. This decision was made as none of the earlier designs tested met the expected moment produced in competition, and the team found that having a heavier foundation that is stable would provide more points than otherwise.

3 Design Objectives

3.1 Turbine Objectives

Looking at the three tasks that will be completed at competition that are specifically focused on the turbine, the team developed design specific objectives to optimize performance in each task. For the power curve performance task our turbine must produce maximum power between wind speeds of 5 m/s to 11 m/s. To accomplish this task, the team's main design objective is to maximize the turbine's coefficient of power. In order to meet this design objective, the team designed blades that maximize the lift coefficient to drag coefficient ratio at the expected Reynolds numbers based on the known wind speeds. The blade shape also maximizes the swept area, optimizing the energy captured from the wind. While the cut-in wind speed is not a measured task in the competition, the team is cognizant of our turbines cut-in wind speed and is aiming to have turbine startup in wind speeds less than 5 m/s. The turbines pitching system will reduce the cut-in wind speed, as well as improve the power output between 5 m/s to 11 m/s.

For the safety task, the wind turbine must be able to reach "shutdown" at wind speeds up to 22 m/s [1]. The design objective for the safety task is to have a braking system that can overcome the moment

created by the shaft at 22 m/s. The team accomplished this design objective by designing a disk brake system that works in conjunction with the pitching system. The pitching system in the stall position slows the rotation of the blades while the disk brake can further decelerate the turbine as necessary.

The durability task of the competition measures the change in foundation position after the completion of the previously mentioned tasks. The main design objective for this task is to minimize the drag on the nacelle and the tower. The design objective was accomplished by creating the most compact nacelle assembly possible. The team further reduced drag by creating a streamline attachment for the tower and the nacelle, thus minimizing the pressure drag.

3.2 Foundation Objectives

There are two tasks targeted towards the foundation, these being the durability task and the structure weight task. The first objective is to create a foundation that would move no more than 6mm during wind tunnel testing. The second objective was to make the foundation as light as possible while still fulfilling the durability objective. Lastly, the foundation must be fully installed within the 15 minutes of allotted time.

Ultimately, the team prioritized durability as this was more crucial to the safe operation of the turbine. Multiple lightweight foundation designs were tested, but the team determined that these lightweight designs did not fulfill the durability objective.

4 Blade Design

4.1 Geometry & Airfoil Selection

In order to design and analyze blades, the team used a Matlab code based on Blade Element Momentum theory (BEM). This code was created by the team and output initial chord lengths and angles of twist at each blade section. The twist angles and chord lengths as a function of radial position can be seen in Figure 3:

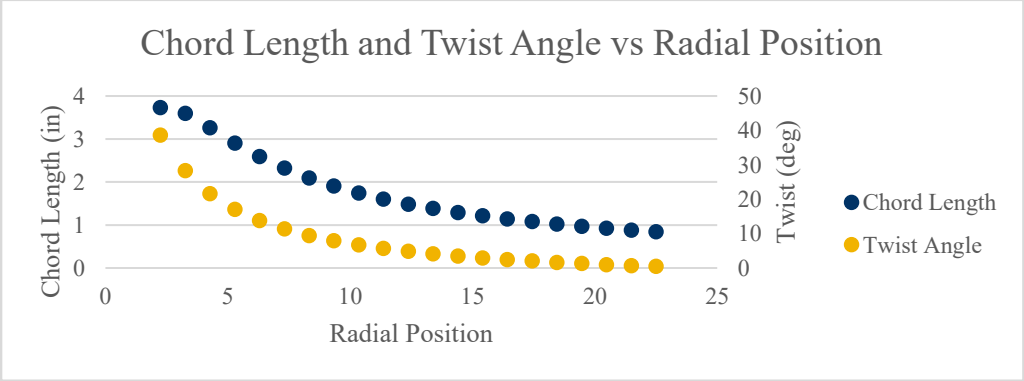

Figure 3: Chord Length & Twist vs Radial Position on the Blade

With these values, the Reynold's number range was calculated for the expected conditions at competition. The Reynold's number was used to evaluate various airfoils that were subsequently simulated using Q-Blade. This simulation data was used to estimate the Power Curve Performance Task score at competition. As a result of this process, the team settled on the GOE79 airfoil as it provided the best balance of manufacturability and performance [2].

4.2 Aerodynamic Analysis

Q-Blade simulations were used to estimate the Coefficient of Power, or Cp, of the blades at various tip speed ratios, or TSR's. As a result of these simulations, the team found a maximum Cp of approximately 0.44 at a TSR of 4.5. Additionally, due to the inclusion of an active pitching system in this year's turbine, Cp vs TSR curves were simulated for a variety of pitch angles relative to this maximum. These curves are overlayed in Figure 4 to visualize the change in performance for varying pitch angles and the ability to feather to turbine blades out of the wind. Similarly, the power curve from 5m/s to 22m/s was generated using simulations from Q-Blade. The rated power for the turbine is 54.3W as seen in Figure 5.

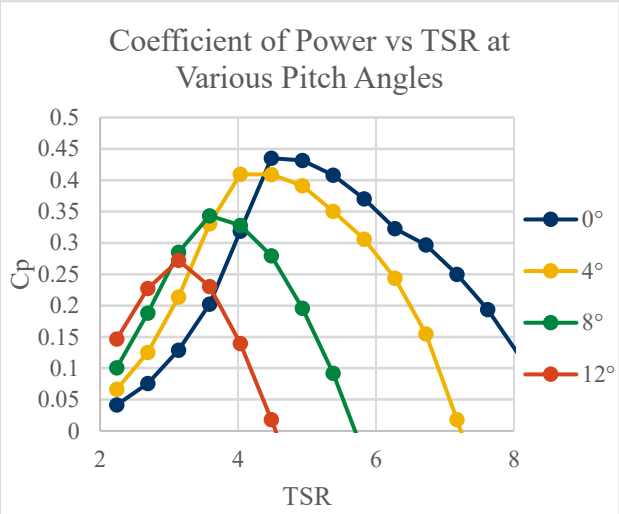

Figure 4: Power Coefficient vs Tip Speed Ratio at Various Pitch Angles

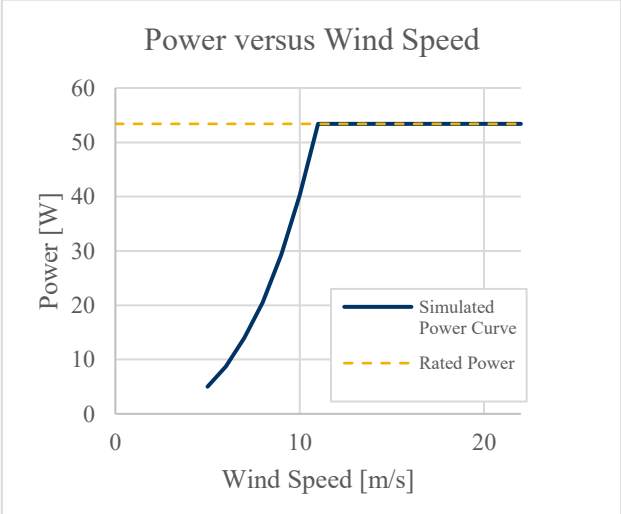

Figure 5: Power [W] vs Wind Speed [m/s]

4.3 Composite Manufacturing

After printing prototype blades, it was determined that fully 3D printed blades would not be suitable for the expected loads given the low percent thickness of the airfoil. After discussions with the composites sponsor, Gurit, the team decided to use BComp, a material similar to carbon fiber but sustainably made from flax seed. Without composite manufacturing experience, the team initially experimented with 3D printing split molds. However, due to the time commitment of designing and manufacturing new molds for every iteration of the blade design, the team decided to switch to vacuum bagging BComp around 3D printed cores. After countless attempts, the desired blade quality was eventually achieved through this method. The manufacturing process first involves hand laying-up the BComp around the cores, placing the blades in a sandwich of peel ply and breather fabric, and sealing the blades in a vacuum bag. Once the blades are removed, they are trimmed and additional coats of epoxy are applied to reach the desired surface finish.

The final blades have both a layer of unidirectional fabric and twill wrapped around a PLA core with a steel grommet inserted into the hub mounting point. The manufacturing process can be seen in Figure 6 with a final blade in Figure 7:

Figure 6: Blade Manufacturing Process

Figure 7: Final Blade

4.4 Blade and Hub Stress Analysis

Due to the complex nature of the composite blades, the team decided to do load calculations only on the mounting point and perform a series of tests on the rest of the blade structure. The load calculations were performed using the mass of the blade, location of the center of mass, and maximum angular velocity in order to find the maximum centripetal force. Using these calculations and the material properties provided by Gurit for the BComp fabric, the team estimated a factor of safety of 1.61.

In order to verify this factor of safety, the team mounted the entire shaft, hubs, and initial blades into a dynamometer and spun the blades until failure. The blades failed at 5306.1 rpm in the location expected, giving the blades a factor of safety of 1.3. As a result of this test, the team decided to alter the geometry of the blade by increasing the distance between the bottom of the blade and the mounting hole as well as imbedding a steel grommet to dissipate the centripetal load.

Figure 8: Blade Centripetal Force Testing Apparatus

Figure 9: Blade Centripetal Force Test Results

In addition to the centripetal test in the dynamometer, the team conducted a bending test. The blade bending test was completed by attaching a weight to the blade tip as seen in Figure 10. The calculated maximum bending stress was 255.02 kPa at 22 m/s, and the testing resulted in a bending stress of 1116.8 kPa before ending the test. This results in a factor of safety of at least 4.38 since blade failure was not reached.

Figure 10: Blade Bending Stress Testing Apparatus

The team also conducted separate hub tests in order to find a factor of safety for the hubs themselves. This was done by mounting weights at a known radius from the attachment point of the hubs and spinning them to a known angular velocity. Similar to the axial blade test, failure was not able to be reached. Due to limitations in the maximum dynamometer angular velocity, the hubs experienced a maximum of 721.2N of centripetal force, yielding a factor of safety of 12.1.

5 Foundation Design

5.1 Initial Axial Thrust and Tower Drag Calculations

When first prototyping foundation designs, the team needed an estimated of the loads the foundation must withstand in the conditions of a runaway event up to 22 m/s. The main sources of these forces were assumed to be the axial thrust of the turbine, the nacelle drag, and the drag on the tower as seen in Figure 11. These forces were estimated with the following equations:

$$T = \frac{1}{2}\rho A U^2[4a(1-a)] \quad \text{Eqn 1}$$

$$F_D = \frac{1}{2}\rho A U^2 C_D \quad \text{Eqn 2}$$

The axial force was estimated with equation 1, where T is the thrust force, ρ is the density of the air, A is the rotor area, U is the free stream velocity, and 'a' is the axial induction factor [2].

Operating at the Betz limit with 'a' = 1/3, sea level density $\rho = 1.23\frac{kg}{m^3}$, rotor area $A = \frac{\pi}{4}D^2$, and free stream velocity $U = 22$ m/s the maximum axial thrust force was calculated to be 42 N or 9.45 lbf. This procedure was done again using the power coefficient of the blades calculated through QBlade. The axial induction factor 'a' was then calculated to be 0.151, and thrust was solved for. MATLAB was used to create a plot of the estimated thrust forces from 0-22 m/s, shown in Figure 12. According to the QBlade limit, the maximum thrust force is 24 N, or 5.4 lbf.

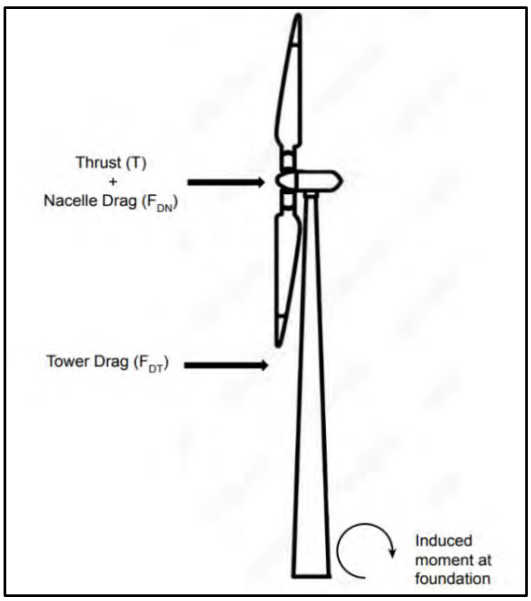

Figure 11: Nacelle and Tower Forces Diagram

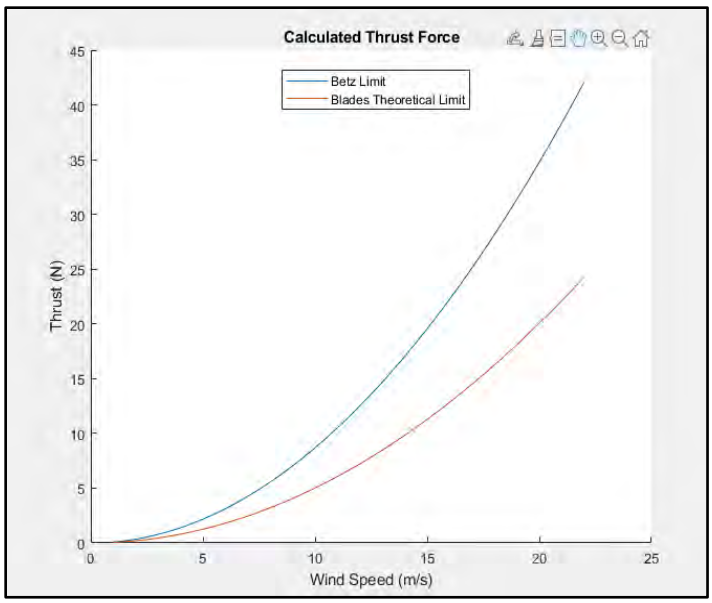

Figure 12: Thrust Force Testing Results

For the initial tower drag estimate, the team used equation 2, where C_D is the coefficient of drag, and A is the planform area of the cylinder. Initially, the tower was assumed to be a cylinder of 3.81 cm diameter with a height of 60 cm. At 22 m/s, the Reynolds number was calculated to be $5 * 10^4$, giving an estimated C_D of 1.1 [3]. Under these conditions, F_{DT} was estimated to be 7.5 N, or 1.7 lbf.

Lastly, the nacelle drag, or F_{DN}, was estimated. This was determined by modeling the nacelle as a simple cylinder of 10 cm diameter perpendicular to the wind, with a C_D of 1.2. Following equation 2 again, this gives a drag force of 2.8 N, or .63 lbf.

With these forces, the tipping moment at the foundation was calculated to determine the restoring moment needed to prevent the tipping of the foundation and turbine. Based on the estimated distance from the rotor center to the top of the sand as 1 m in the competition rules, the distance from the center of the tower would be approximately 0.7 m. By multiplying the forces with their respective lengths, the calculated maximum theoretical moment is 50 N*m, or 37 lbf*ft. Using the maximum Cp from Q-Blade, the maximum theoretical moment is 32 N*m, or 23.6 lbf*ft.

5.2 Axial Drag Reductions

After the initial forces were estimated, the team investigated ways to reduce these forces. Since the majority of the torque produced is from the thrust force of the rotor, the team looked at ways to reduce this thrust force. However, it was found that this would result in decreased performance in the power curve performance task. The team decided to prioritize decrease the drag on the nacelle and tower in order to improve the foundation durability without sacrificing power output.

To accomplish a reduction in drag on the tower, the team decided to create a streamline attachment to slide over the tower to reduce the pressure drag. The streamline chosen was an EPPLER 863 strut airfoil. This was chosen for two reasons. The first was due to the high percent thickness, allowing the full length of the airfoil to fit within the 15cm tower diameter requirement. A top view of this attachment can be seen in Figure 13. The second reason was the relatively low drag coefficient, minimizing the load on the foundation.

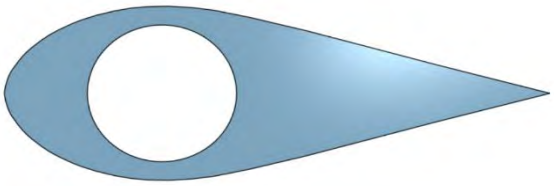

Figure 13: EPPLER 963 Airfoil Tower Attachment

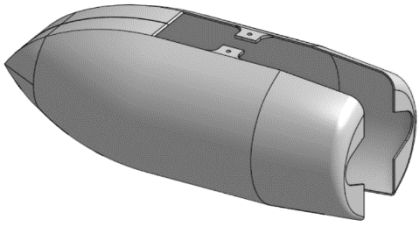

Figure 14: Streamlined Nacelle Covers

Similarly, the nacelle was also streamlined to reduce pressure drag. This was done through creating covers that tapered down to a point, mimicking the design of an airfoil, seen in Figure 14.

5.3 Load Cell Testing

To better determine the forces the foundation will be subject to, the team decided to devise a test to measure the horizontal drag forces. This was done through using a 10 kg load cell attached to the bottom of an extended tower that was designed to pivot about an axle. The turbine would then push against the load cell in the opposite direction of the incoming wind as seen in Figure 15. To calibrate the load cell, the team used a scale to pull at a known weight and inputted the value into the Arduino calibration code.

With this testing set up in combination with a cup anemometer, the team is able to estimate the drag forces on the turbine. After having done initial tests, the team noted that the maximum thrust output at approximately 15 m/s was on the order of 2 lbf, or 9 N. Referring to Figure 12 in section 5.1, this is slightly lower than the blades theoretical limit.

It should be noted that there are a few limitations with the current testing setup, mainly that the tower length above the pivot point is not identical to the competition tower length, and the drag on the tower below the pivot point will counteract the thrust force. Additionally, it was noted that the turbine created vibrations that are not easily replicable when testing the foundation.

Figure 15: Axial Thrust Force Testing Apparatus

5.4 Design Iterations

At the beginning of foundation testing, the team focused on the structure weight portion of testing. The first foundation prototype was a mesh box design intended to resist the predicted thrust force of 42 N. Due to the uncertainty of the sand properties, the team determined that it was essential to immediately begin testing procedures. After building the mesh prototype and testing apparatus similar to the one that will be present at the competition, foundation testing data could be collected. The mesh design resisted less than 4 N of force acting at the location of the hub and was therefore redesigned for a better performance.

The next design iteration made use of multiple “sand screws” that would be inserted into the ground and intended to maintain the stability of the foundation. 3D printed sand screws of various geometries were

created for testing purposes. After conducting similar testing to the mesh box, the team found that none of the sand screws designed were able to resist the estimated thrust loading.

The third design iteration was a steel box that would be inserted into the sand depth and then filled with sand to act as a weighted foundation. Multiple box geometries were created and tested including a box design with an angled backplate that was intended to make use of compressive forces in the sand. The highest amount of blade thrust force the box designs could resist was 11 N. The team tested the same steel box design and added 37.5 lbs of weights to the box. The weighted box resisted 42 Nm which had the best performance.

The design iteration process began with several lightweight structures that did not perform as well as anticipated. Due to potential improvements in the overall points scored at competition as well as preventing possible damage to the turbine, the priority shifted from weight reduction to durability.

The final design consists of a 25 x 25 cm 3/16 in thick steel plate with a 1.5 in steel tube welded to the center. Two threaded rods were then welded to the front half of the steel plate. Multiple 25 x 10 x 2.5cm steel blocks had holes drilled through them to allow them to fit over the threaded rods. A total of six blocks can be added, giving a final weight of 70 lbs, or 31.7 kg. Based on the maximum moment of 32 N*m calculated in Section 5.1, the factor of safety against tipping for this design is 1.84.

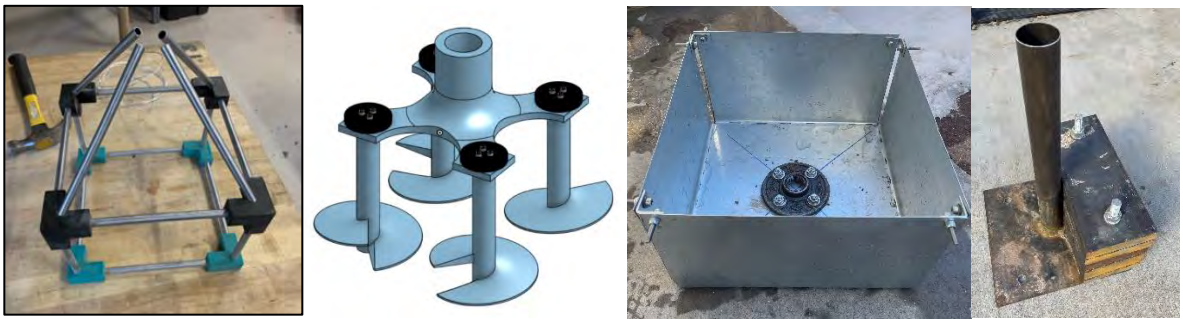

Figure 16: Foundation Design Iteration Method from Oldest (Left) to Most Current (Right)

5.5 Installation Procedure

The competition requires that the foundation design be installed into the testing facility without any of the team members' hands touching the water. For the installation process, the team has designed a square steel perimeter box (Figure 17) that slides into the sand. The steel perimeter box is dimensioned with an opening of 25 x 25cm that fits around the foundation and extrudes out of the water, allowing the team to hold onto it without touching the water. This installation tool also contains markings near the top of the waterline that depict how far into the sand the box should be installed.

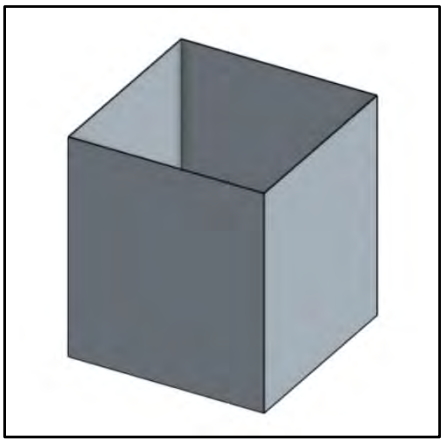

Figure 17: Installation Perimeter Box

The first step of installation is sliding the installation perimeter box into the sand until the waterline reaches the indicated marking. A long shovel is then used to dig out the sand within the box without touching the water. The sand removed from inside the box is simply dumped outside of the box. Once the team has dug out all the sand to the bottom of the perimeter box, a garden hoe is then used to remove any sand in the corners of the box. The garden hoe is

also used to pack down the sand at the bottom of the box and creates a flat surface for the foundation to rest. The foundation is then lifted by a team member and carefully dropped into the perimeter box until it is fully resting on the sand at the bottom. The perimeter box is then slid out of the sand and the excess sand surrounding the foundation is compacted. This completes the installation process.

5.6 Foundation Testing

The foundation was subjected to one test, a moment arm test. The foundation was installed as the team plans to do in competition. Then a fish scale was attached to the top of the tower, where the thrust force from the nacelle will act on the tower. The scale was then pulled until the tower moved more than 6 mm; the force needed to move the tower was recorded. The moment arm test was completed for every foundation design concept our team built.

Figure 18: Foundation Testing Setup

6 Mechanical Design

6.1 Nacelle

The nacelle is designed to provide mounting locations for both linear actuators, the generator, the shaft bearing, the linear bearings, the covers, and tower connection. The design went through two main iterations from the first to the second semester. The initial design consisted of a flat plate with slots to provide easy modification and design flexibility when designing the mounts for all subsystems. Once the team had decided on the overall nature of each subsystem, the nacelle went through a complete redesign.

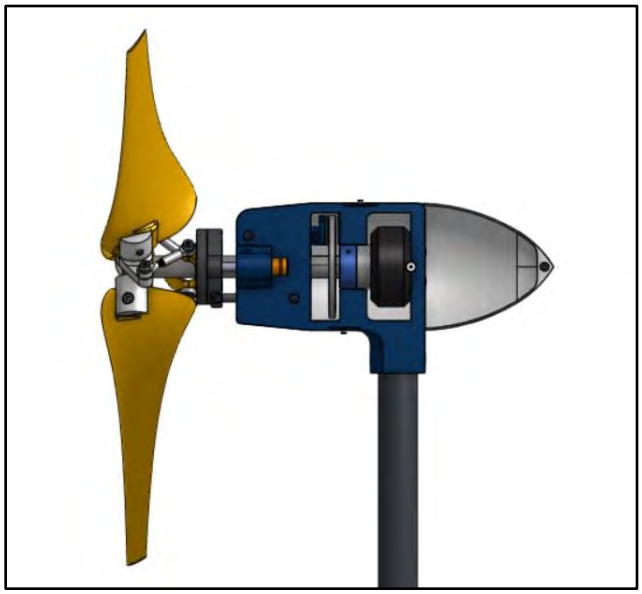

Figure 19: Wind Turbine Full CAD Model Internal View

This redesign was focused on reducing the size and part count of the turbine. Size reduction was prioritized in order to reduce the axial drag on the nacelle, and thus reduce the load on the foundation. The tower mount was also shifted towards the back of the nacelle in order to keep the mass of the turbine in front of the foundation's point of rotation. The current nacelle consists of only two 3D printed parts with various heat-set inserts used in order to provide reliable threads for subsystem attachment. The rear of the nacelle provides the mounting locations for the tower, generator, and stationary brake pad while the front holds the shaft bearing and linear bearings for the pitch system. Both actuators are imbedded within the front of the nacelle and various channels were designed to provide adequate cable management.

6.2 Pitching

The pitching system is designed to change the angle of all three blade simultaneously. The system will be used to prevent aerodynamic hysteresis and add redundancy to the braking system. The system is comprised of a linear actuator, a linear swash plate, three push rods, and three blade hubs. The blades are connected to the shaft via the hub pieces as seen in Figure 20, and these parts allow the blades to rotate around the bolt attaching the hub to the shaft. The push rods attach the hubs to the linear swash plate. The push rods are made up of two ball joints at each end of the rod, the ball joints allow the geometry of the system to change when pitching. The linear swash plate allows the inner disk to rotate with the rotation of shaft while holding the outside side steady in order to attach it to the linear actuator. The linear actuator is mounted to the nacelle and the piston rod is mounted to the linear swash plate. As the piston rod extends and retracts the blades all change angle in unison.

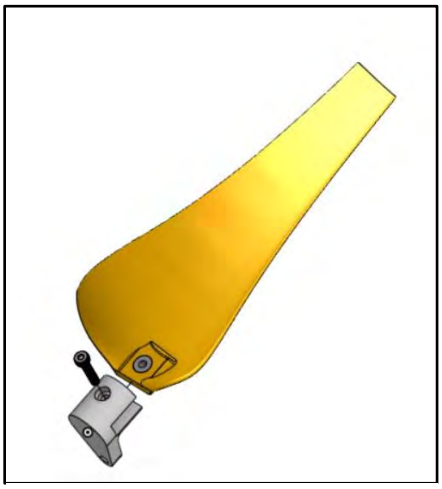

Figure 20: Blade and Hub Assembly

The entire system is controlled with a single linear actuator which means that the linear actuator chosen for the system must be able to withstand the force acting on it from the pitching moment. In order

to calculate the pitching moment created by the blades, the team had to first complete an analysis of the pitch mechanism geometry.

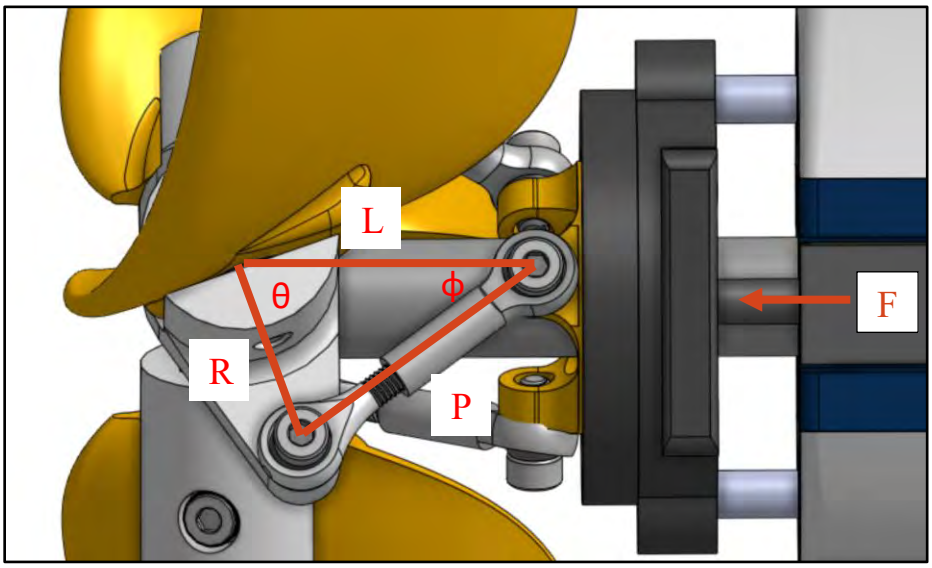

Figure 21: Pitching System Geometry

As seen in Figure 21, the pitch system has a constant hub length, R, and push rod length, P, but changes in length on the shaft, L, due to the change in the linear actuator piston rod length. The change in length causes the angles θ and φ to also change. The change in φ can be described using Equation 3. The total force can then be described using Equation 4, where M is the pitching moment for one blade. The force equation is specific to the geometry of the system. Once the previous two equations were developed, the total pitching moment for one blade was calculated elementwise using Equation 5.

$$\varphi = cos^{-1}\sqrt{1-(R/L)^2 \sin(\theta)^2} \qquad \text{Eqn 3}$$

$$F = \frac{3Mcos(\varphi)}{Rcos(90-\theta-\varphi)} \qquad \text{Eqn 4}$$

$$M = C_M(1/2)q_\infty {U_{rel}}^2 Ac \qquad \text{Eqn 5}$$

The variables in the Equation 5 are defined as follows: C_M is the moment coefficient of an airfoil at a specific Reynolds number, q_∞ is the dynamic pressure, U_{rel} is the wind speed relative to the blade, and A is the chord length, c, times the span, S. The geometry of the blade was gathered from the program QBlade, and the moment coefficient was gathered from Airfoil Toolbox [4] for a GOE79 airfoil. The team then calculated the relative velocity of the wind at each section of the blade, followed by calculating the pitching moment at each section of the blade. The air density was assumed to be standard air density at sea level. The following table shows the elementwise calculations for one blade:

Table 1: Blade Pitching Moment Analysis

	Blade Section	Chord Length (m)	Section Arean (m^2)	Local TSR	U relative (m/s)	Section Pitching Moment (Nm)
1	1	0.0491	4.9056e-04	0.5998	25.6540	0.0010
2	2	0.0523	5.2307e-04	0.8314	28.6103	0.0014
3	3	0.0511	5.1087e-04	1.0630	32.1073	0.0016
4	4	0.0480	4.8046e-04	1.2946	35.9879	0.0018
5	5	0.0445	4.4482e-04	1.5261	40.1410	0.0020
6	6	0.0410	4.0964e-04	1.7577	44.4902	0.0020
7	7	0.0377	3.7715e-04	1.9893	48.9834	0.0021
8	8	0.0348	3.4798e-04	2.2209	53.5844	0.0021
9	9	0.0322	3.2209e-04	2.4525	58.2676	0.0022
10	10	0.0299	2.9921e-04	2.6841	63.0148	0.0022
11	11	0.0279	2.7898e-04	2.9157	67.8124	0.0022
12	12	0.0261	2.6105e-04	3.1472	72.6505	0.0022
13	13	0.0245	2.4510e-04	3.3788	77.5215	0.0022
14	14	0.0231	2.3086e-04	3.6104	82.4196	0.0022
15	15	0.0218	2.1808e-04	3.8420	87.3402	0.0022
16	16	0.0207	2.0657e-04	4.0736	92.2798	0.0022
17	17	0.0196	1.9616e-04	4.3052	97.2353	0.0022
18	18	0.0187	1.8671e-04	4.5368	102.2046	0.0022
19	19	0.0178	1.7810e-04	4.7683	107.1856	0.0022
20	20	0.0170	1.7021e-04	4.9999	112.1769	0.0022
21	21	0.0163	1.6298e-04	5.2315	117.1771	0.0022

The summation of the pitching moment on each section of the blade was then used in the previous force equation with the system geometry to find the total force required for our linear actuator. Figure 22 describes the force required for the range of angles in our system.

The greatest force the linear actuator is required to hold is 11.17 N. The linear actuator being used is the PQ12-100-6-R Micro-Actuator. This linear actuator has a hold force of 50 N, giving the system a factor of safety of 4.48.

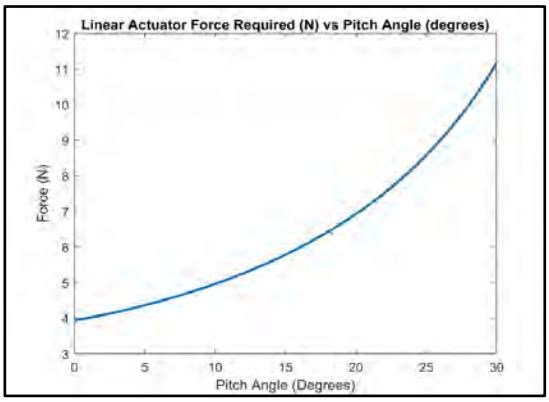

Figure 22: Linear Actuator Force Required vs Pitch

6.3 Brakes

The brakes use a linear actuator with a mounted brake pad to press against a sliding brake disc, compressing the disc with a secondary brake pad fixed to the nacelle. The actuator pad uses a 3D printed mount and both brake pads are made of neoprene rubber. The aluminum disc was manufactured using a CNC router. The chosen actuator is a micro linear servo capable of producing 50 N of force. The brake disc has a diameter of 7.2 cm giving the turbine a theoretical braking force of 3.6 N-m. The design was chosen by the equations for angular momentum and impulse.

The brake system also underwent two different tests: a static test and a dynamic test. The static test had the brake engaged and weight added to the radius of the disk brake. The weight on the radius of the disk brake created a moment on the system. Weight was added until the brake failed, in turn allowing the shaft to spin. While the static test did not show that the brake provided adequate force for the system, the dynamic car testing showed that the system sufficiently decelerated and could

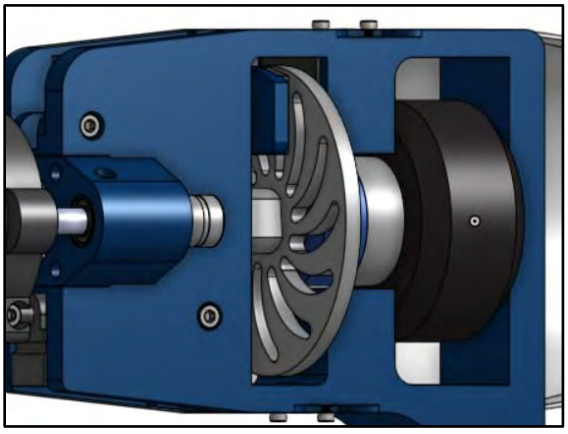

Figure 23: CAD Disc Brake Mechanism

withstand 22 m/s winds without brake failure. The team theorizes that this is due to rapidly decreasing the TSR of the blades and thus reducing the torque generated by the blades.

Figure 24: Static Brake Testing Apparatus

6.4 Tower and Yaw

The tower has been welded to a 0.5-inch-thick steel baseplate. In order to ensure that the weld can resist the forces acting on the tower, a load analysis was conducted to determine the minimum throat length of the weld necessary to maintain structural integrity. The forces acting on the tower were assumed to be equivalent to the axial thrust forces at the location of the nacelle (calculated previously as 42N). The force acting at the top of the tower, the diameter of the tower and the ultimate tensile strength of the welded material were used to estimate the specific weld size. The direct shear stress and bending tensile stress were calculated from Equations 6 and 7 and then combined in Equation 8 for a resultant stress at the weld location [5]. Eq. 9 was then used to find the minimum throat length to resist the estimated force.

$$\tau_s = \frac{Force}{Unit\ Throat\ Length} \quad \text{Eqn 6}$$

$$\tau_b = \frac{Moment * Y}{Unit\ Moment\ of\ Inertia} \quad \text{Eqn 7}$$

$$\tau_r = \sqrt{{\tau_s}^2 + {\tau_b}^2} \quad \text{Eqn 8}$$

$$throat = \frac{\tau_r}{Design\ Strength} \quad \text{Eqn 9}$$

From the above calculations it was determined that having a throat length of 3mm on for the weld will result in a factor of safety above 15. The team assessed this as adequate for maintaining the structural integrity of the tower and baseplate and moved forward with the weld design.

The yaw system is a simple bearing surface with a pin to prevent rotation after foundation installation. A loading force acting on the nacelle is expected to occur and cause stress at the location of the yaw. The team needed to assess the amount of force that could be placed on the yaw without causing the nacelle to fail. Through testing (Figure 25), the nacelle yaw was able to resist approximately 222 N of force. Compared to the expected thrust force acting on the nacelle of 42N, this is a minimum factor of safety of 5.

Figure 25: Nacelle Yaw Loading

7 Electrical System Design & Analysis

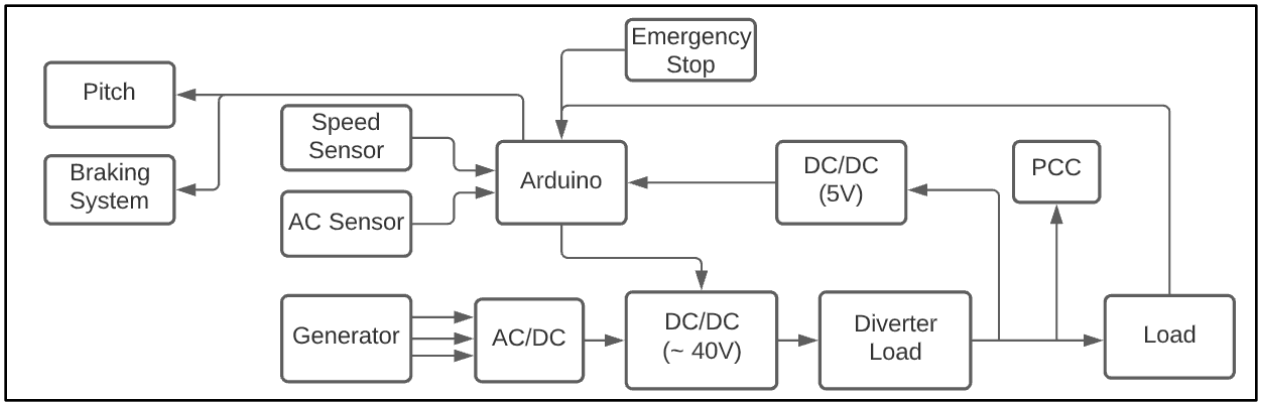

Figure 26: Electrical System Architecture

7.1 Generator

The selected generator for the electrical system was the MAD IPE 5012 160kV motor. The relatively low kv rating of the motor allows for the team to utilize a boost converter for all windspeeds expected at competition. The motor's higher efficiency than competitors at low RPMs made it an ideal candidate for selection in our design for the competition. Additionally, it only reaches about 54 °C after 5 minutes at maximum power output, which was significantly lower than that of its competitors [6].

7.2 AC/DC

A three-phase full wave bridge rectifier, Figure 27, is used to convert the three-phase output of the generator into a DC voltage. The DC voltage then goes through a capacitor of 10µF to help reduce the ripple created by the rectifier. This unit was purchased to help reduce the power losses compared to building one with 6 individual diodes.

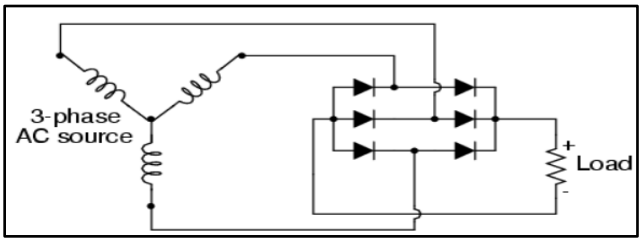

Figure 27: Three-Phase Full-Wave Bridge Rectifier

7.3 DC/DC Boost Converter

The main system is the DC/DC boost converter, Figure 26, this system consists of: 98.5µH inductor, N-channel power MOSFET, diode, and 100µF capacitor. The microcontroller in our system is the Arduino MEGA 2560 coded with MATLAB Simulink. The Arduino will take the output voltage from a voltage divider connected to the output of our system. Depending on the output voltage the duty cycle of the square wave going into the MOSFET will change from 20% to 60% as shown in Figure 28. This control in the duty cycle allows the voltage at the output to be controlled and limited to a maximum of 40 V.

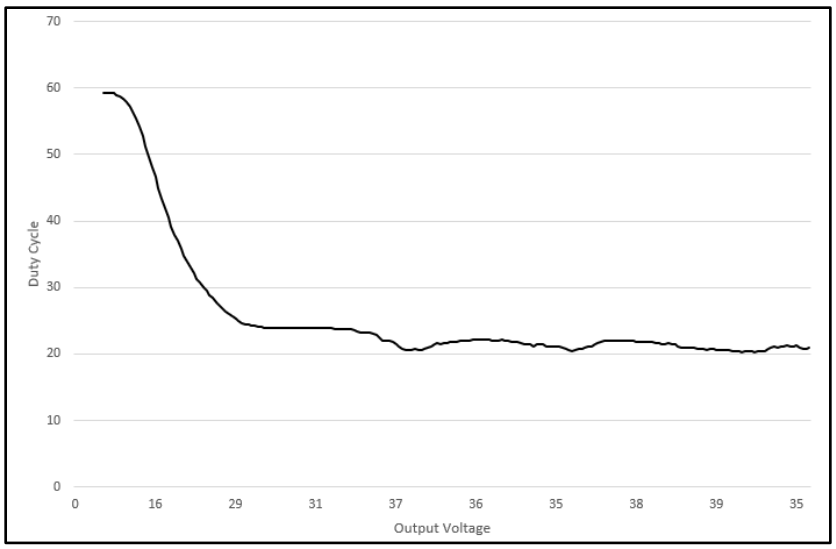

Figure 28: Duty cycle compared to Output Voltage

7.4 Diverter Load

Another important electrical system is the diverter load, Figure 26. The diverter load consists of twelve 10 Ω 100W rated resistors to make an equivalent resistance of 4Ω at 1200 W. This system is controlled by an N-channel power MOSFET used as a switch. The Arduino takes the output voltage and current sensor data to determine if a signal needs to be sent to the gate. If the current is zero, that indicates that the load is disconnected and the MOSFET will turn on, giving power to the diverter load. Within the Simulink code, power is also calculated. If output power reaches a certain value, in our case 40V to give the system some error before reaching the competition maximum of 48V in the case of a runaway or quick RPM boost, the MOSFET will turn on to not exceed that power output. Along with the DC/DC boost converter, this system will also regulate the system voltage when needed. It regulates the power of the system through the dissipation of heat into the large heat sink as seen in Figure 29.

Figure 29: Diversion Load

7.5 Printed Circuit Board

The system in Figure 26: Electrical System Architecture, is implemented onto a PCB. Wire connections are used for the generator, Arduino, diverter load, DC/DC buck converter, and load. The AC/DC Converter, DC/DC boost converter, and sensors are built onto the PCB. All the components on the PCB are through-hole compatible since through-hole components are easier to find higher rated devices for. The PCB is a 2-layer design with top traces shown in red and bottom traces shown in blue as seen in Figure 30. The traces are 1.02 mm equivalent to 18 AWG allowing the board to be rated for 10 Amperes. The board was purchased through JLC PCB.

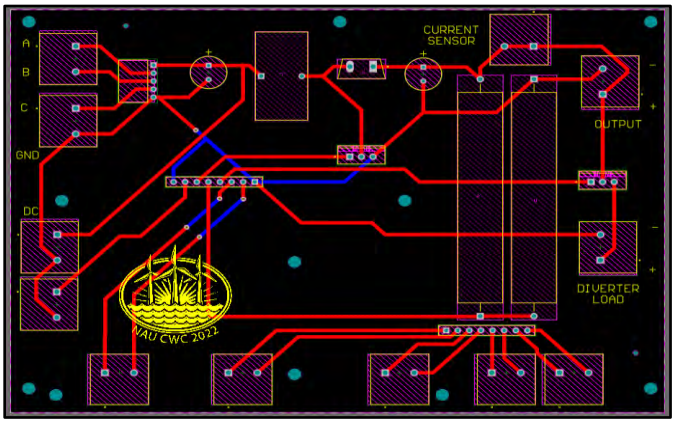

Figure 30: Electrical System Architecture

7.6 Load

The load for the system will be a power resistor capable of 200 W and around 2 Ω. When testing the system at different resistances such as: 15 Ω, 10 Ω, 4 Ω, and 2 Ω. It was found that at lower resistances the current drawn from the source and output current was much larger than when testing at higher resistances. Since the output current for our system can be a maximum of 10 A, the resistance of 2 Ω allows the most current: increasing our power output and efficiency.

8 Software Implementation and Testing

8.1 Software

The program that was used to control all electrical systems and the boosting of the boost converter was all done through MATLAB Simulink. Simulink allowed us to use block style programming and Arduino addon which helped make hardware uploading to the Arduino quite easy, this also helped make it easy to write the algorithms and was able keep everything clearly organized using subsystems for the various parts of the control system for the turbine shown in Figure 31. For testing, we

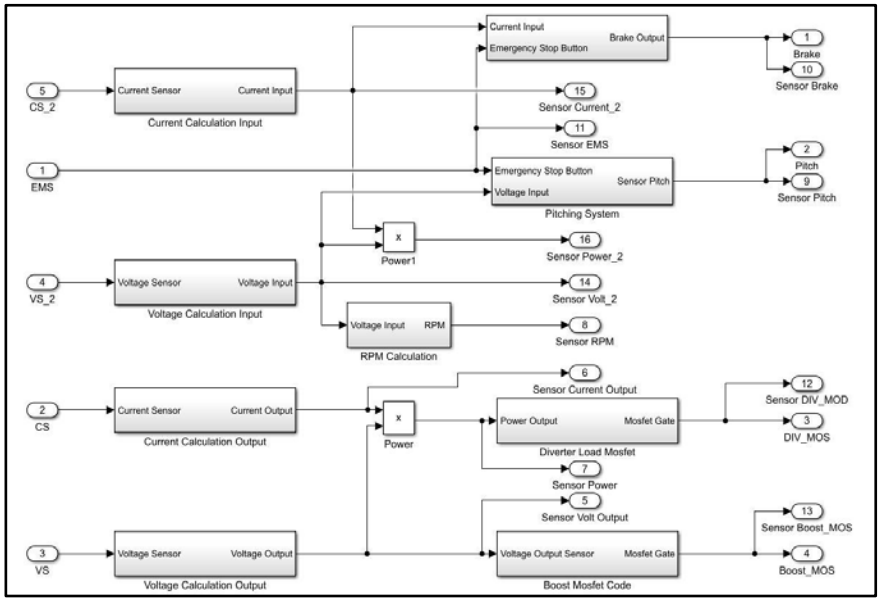

Figure 31: Main Control System Design

used sensor outputs that went to scopes in Simulink to help monitor the input and output data going to the Arduino. And we used another Arduino that read the actual pins going in and out of the main control Arduino and logged the data on an Excel spreadsheet.

9 Field Testing

9.1 Procedure

Before the completion of the full turbine testing, our team tested each subsystem individually. Each individual test allowed our team to gain a better understanding of what is to be expected in the full turbine test. The individual tests also provided our team with a factor of safety for each system, ensuring that each system will be strong enough before assembly. Each of the subsystem tests were completed multiple times to reduce random error with the exception of the tests that resulted in broken parts.

Figure 32: Car Testing Apparatus

Once the team completed individual tests for each subsystem and felt confident in the results gathered the team moved to full turbine testing. The full turbine test proved to be a challenge due to the wind tunnel at NAU not having a large enough test section for our turbine. As mentioned previously, our team designed and built an apparatus to mount our wind turbine on top of a car for testing as seen in Figure 32.

In preparation for car testing, our team assembled the entire turbine and mounted it to the testing apparatus, which was then mounted to the roof of a car. The wires for the motor and the two linear actuators were fed down the tower and into a window of the car. In the car, our team had all the electrical components, including our boost system, control system, and a PCC. A cup anemometer was also mounted in order to collect wind speed data. The PCC recorded the wind speed, voltage, and current of the turbine during each test. The pitch angle and the electrical resistance were changed independently, and values were recorded to compare the power output at various pitch angles and resistances. The axial drag induced on the foundation by the turbine was also tested in this system using the load cell discussed in section 5.3. The team then recorded the thrust force on the nacelle at wind speeds up to 22 m/s. The data provides an estimate for the moment that the turbine will experience at competition.

9.2 Results

During the car testing performed on the entire turbine system, the blades, pitch, brakes, and force acting on the foundation were assessed. Before car testing began, individual tests were conducted on the turbine subsystems to prove the durability and safety of each system. The following discussion determines the reliability and functionality of the designed wind turbine.

The primary form of testing conducted by the team was through car testing. The blade performance, pitch degree performance, and braking performance were all analyzed by this test. In addition to testing the individual subsystems, the overall functionality of the turbine was evaluated. All the subsystems were able to work in unison during car testing to generate power, resulting in a functional turbine. The pitch angle of the blades was changed to find the angle that would generate the greatest amount of power. The pitch angle for startup speeds and slow down speeds were also determined through car testing. It was determined that

the turbine could be completely stopped through the pitching mechanism. This reduces the rotation of the blades and allows for the disc brake system to act as an additional brake for safety purposes.

10 Changes from Last Year

This year's team was not involved with the design and construction of last year's turbine, so much of the current design is new. The four main subsystems that were inspired by previous years were the pitching, braking systems, and electrical system of last year and the composite blades from the 2014 team.

The pitching system from 2021 was designed around the traditional swash plate mechanism but was driven by a motor geared to a rack and pinion system. After discussions with the graduates of that team, it was found that they encountered difficulties in supplying enough force to counter the pitching moment of the blades with this design. Additionally, the design took up significant space inside the nacelle body. As a result, the team used the initial swash plate concept but redesigned with nacelle to accommodate a lead screw design initially, and eventually a linear actuator. The sliding disk brake was also inspired by last year, as well as the many other past teams from both NAU and other universities that utilized a similar system.

The electrical system took inspiration from the previous year's team with: the three-phase full wave bridge rectifier, DC/DC boost converter, and resistive load. The main changes for this year were: using MATLAB Simulink to code the Arduino MEGA 2560, designing the diverter load, designing the DC/DC boost converter, and designing a PCB for the system.

The manufacturing process of the blades was initially inspired by the 2014 team's split mold method. However, after initial prototype blades were made using this method, it was found that the process to re-manufacture the molds for new iterations of the blades was extremely time consuming. As a result, the team branched off into vacuum bagging composite material around a 3D printed core as this allowed for both rapid design iteration but also strong and rigid blades. This was an entirely new process for everyone on the team and took a significant amount of trial runs to reach the current state of the blades.

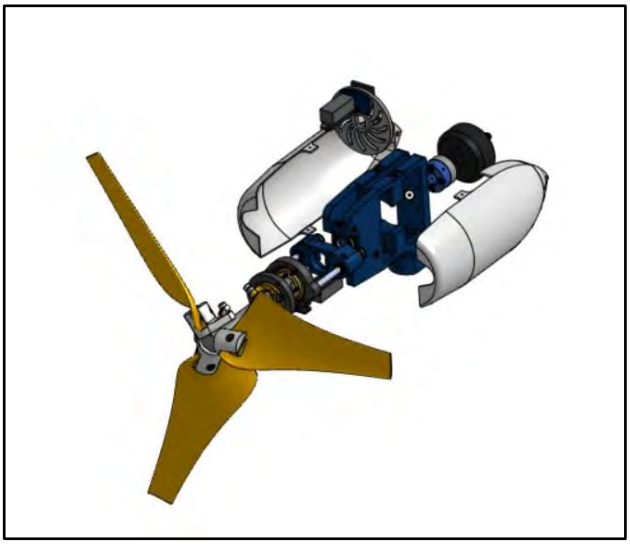

Figure 33: Turbine Exploded View

Figure 34: Assembled Turbine

11 References

[1] "U.S. Department of Energy Collegiate Wind Competition 2022," 14-Oct-2022. [Online]. Available: https://www.energy.gov/sites/prod/files/2020/10/f79/cwc-2021-rules-requirements.pdf. [Accessed: 29-Nov-2021].

[2] J. F. Manwell, J. G. McGowan, and A. L. Rogers, *Wind Energy explained*. Chichester: John Wiley, 2002.

[3] P. J. Pritchard, J. C. Leylegian, R. Bhaskaran, J. W. Mitchell, and R. W. Fox, *Fox and McDonald's introduction to Fluid Mechanics, 9th edition*. Wiley, 2015.

[4] "GOE79 (PFALZ 11) AIRFOIL," [Online]. Available: http://airfoiltools.com/airfoil/details?airfoil=goe79-il

[5] S. Ghosh, "Fillet weld strength calculation example for welded connection subjected to bending," *mechGuru*, 19-Oct-2019. [Online]. Available: https://mechguru.com/free-caculator/weld-strength-calculation-example-for-bending-moment-application/. [Accessed: 24-Apr-2022].

[6] "Amazon.com: Mad components 5012 IPE v3.0 160KV brushless ..." [Online]. Available: https://www.amazon.com/MAD-COMPONENTS-Multirotor-Quadcopter-Hexrcopter/dp/B08K482875. [Accessed: 25-Apr-2022].

12 Appendix/Photo Collection

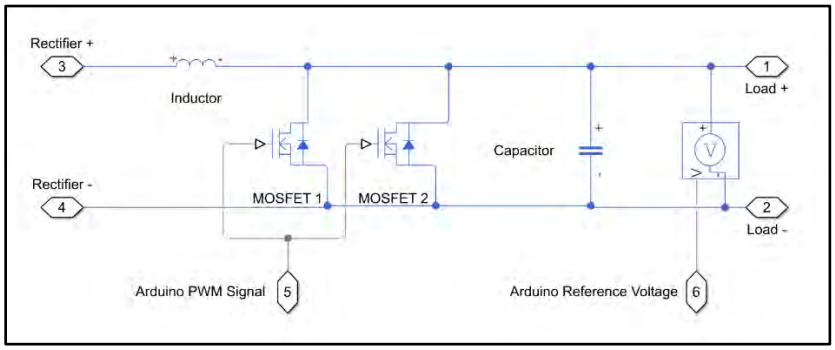

Figure A1: DC/DC Boost Converter

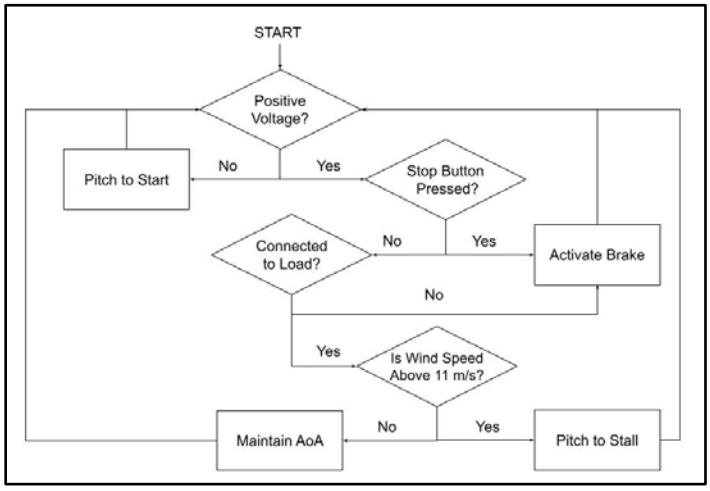

Figure A2: Control Flow Diagram